Porous Silicon Micromachining Technology

Giuseppe Barillaro

Contents

Abstract

In this chapter, silicon electrochemical micromachining (ECM) technology is reviewed with particular emphasis to the fabrication of complex microstructures and microsystems, as well as to their applications in optofluidics, biosensing, photonics, and medical fields. ECM, which is based on the controlled electrochemical dissolution of n-type silicon under backside illumination in acidic (HF-based) electrolytes, enables microstructuring of silicon wafers to be controlled up to the higher aspect ratios (over 100) with sub-micrometer accuracy, thus pushing silicon micromachining well beyond up-to-date both wet and dry microstructuring technologies. Both basic and advanced features of ECM technology are described and discussed by taking the fabrication of a silicon microgripper as case study.

Introduction

Silicon micromachining tools (Köhler 1999) have been developed for over 50 years with the ambition of sculpting silicon wafers at the microscale, continuously paving the way toward novel research/market devices and applications. In the 1960s, the

G. Barillaro (✉)
Dipartimento di Ingegneria dell'Informazione, Università di Pisa, Pisa, Italy
e-mail: g.barillaro@iet.unipi.it

L. Canham (ed.), *Handbook of Porous Silicon*,
DOI 10.1007/978-3-319-05744-6_79

market request for microfluidic devices, e.g., chromatographic columns, inkjet cartridges, etc., drove micromachining research/industry toward the development of wet etching technology characterized by low-cost, but with limited flexibility in fabrication and low integration density. In the 1980s, novel challenging applications, e.g., microelectromechanical systems (MEMS), and lab-on-a-chip (LoC), pushed micromachining research/industry toward the development of dry etching technology with increased flexibility in fabrication and higher integration density, although higher cost too. Both wet and dry technologies are still under development, with wet technology being used nowadays for the fabrication of undemanding microstructures with low density at lower cost, and dry technology exploited for the fabrication of complex microsystems with increased density at higher cost. In the 2000s, the new challenge for silicon micromachining has been the development of high-aspect-ratio technology that allows the etching of microstructures and microsystems with different shapes and micrometer-sized features to be finely controlled up to very high aspect ratios (over 100), thus enabling the actual exploitation of the room available in the third (out-of-plane) wafer direction and breaking novel research/market grounds, e.g., Through Silicon Via (TSV) fabrication for a new generation of three-dimensional chip stacking.

Electrochemical Micromachining of Silicon

Electrochemical micromachining (ECM) (Bassu et al. 2012) of silicon has been recently demonstrated as a powerful and flexible microstructuring technology that allows the etching of silicon wafers to be controlled up to the higher aspect ratios (over 100) with sub-micrometer accuracy, thus pushing silicon micromachining well beyond any up-to-date both wet and dry microstructuring technology. ECM technology capitalizes on the experimental and theoretical results reported in the literature over the last two decades on the electrochemical etching of n-type silicon under backside illumination in acidic (HF-based) electrolytes (backside-illumination electrochemical etching (BIEE)) (Lehmann 2002). The BIEE was pioneered, in the 1990s, by Lehman and Föll for the controlled etching of high-aspect-ratio macropores (Lehmann and Föll 1990; Lehmann 1993, 2002; Foll et al. 2000; Barillaro et al. 2002a; Barillaro and Pieri 2005; Barillaro and Strambini 2010), and later, in the 2000s, pushed by a number of scientists to the fabrication of a multitude of high-aspect-ratio microstructures for different applications (Ottow et al. 1996; Ohji et al. 1999; Kleimann et al. 2001; Barillaro et al. 2002b, 2003, 2005a, b, 2006, 2007a, b, 2008, 2009a, b; Schilling et al. 2001; Matthias et al. 2004, 2005; Astrova and Nechitaĭlov 2008; Astrova et al. 2009, 2010). For a review of the fabrication of macropores by anodization, see handbook chapter "▶ Macroporous Silicon." In the 2010s, a novel dynamic control of the electrochemical etching anisotropy as the etching progresses has allowed the silicon dissolution to be switched in real time from the anisotropic to the isotropic regime and has enabled advanced silicon microstructuring to be performed (Bassu et al. 2012; Barillaro

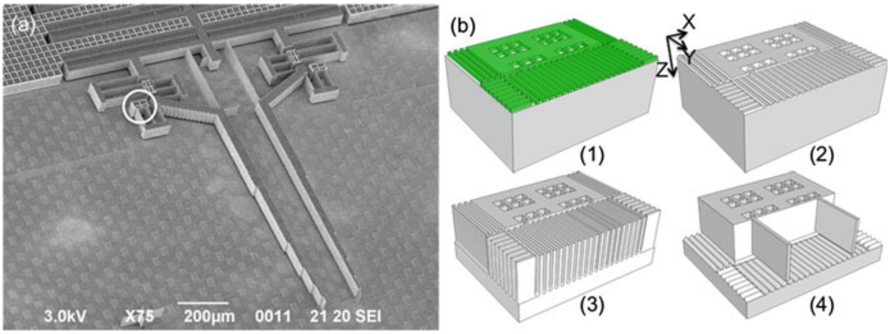

Fig. 1 (**a**) Example (SEM image) of a silicon microgripper fabricated by ECM technology; (**b**) main technological steps for advanced silicon microstructuring by ECM technology, with specific reference to the part highlighted (see *circle*) of the silicon microgripper in (**a**).

et al. 2011; Merlo et al. 2012a, b, 2013; Strambini et al. 2012; Surdo et al. 2012, 2013; Carpignano et al. 2012; Polito et al. 2013).

Fabrication of microstructures and microsystems by ECM technology (Bassu et al. 2012; Surdo et al. 2012, 2013; Polito et al. 2013) is carried out according to the following main technological steps, which are sketched in Fig. 1b with specific reference to the microgripper of Fig. 1a. The starting material is *n*-type silicon, orientation (100), with a thin silicon dioxide layer on top. The pattern of the microstructure to be fabricated is defined on a photoresist layer by standard lithography, transferred to the silicon dioxide layer by buffered HF (BHF) etching through the photoresist mask (Fig. 1b-1), replicated (seed point formation) into the silicon surface by potassium hydroxide (KOH) etching through the silicon dioxide mask (Fig. 1b-2), and finally grooved into the bulk material by BIEE. The BIEE consists of a single-etching step with an initial anisotropic phase (Fig. 1b-3), used to etch the seed pattern deep in the substrate and create high-aspect-ratio microstructures, and a final isotropic phase (Fig. 1b-4), used to release part of the etched microstructures from the substrate and, eventually, yield them freestanding. A dynamic control of the electrochemical etching anisotropy, which is used to switch the silicon dissolution in real time from the anisotropic to the isotropic regime, is synergically combined with the use of both functional and sacrificial structures. Functional (sacrificial) structures are, by definition, parts of the microsystem that are anchored (not anchored) to the silicon substrate after the isotropic phase of electrochemical etching step (and are, hence, removed). The former are indeed functional to the microsystem operation, while the latter are sacrificed for the accurate microsystem fabrication. All the microsystem parts visible in the SEM image of Fig. 1a are functional structures, which are still connected to the substrate through anchor structures properly designed to withstand the isotropic phase of the BIEE. Sacrificial structures are removed after the isotropic phase of the BIEE and hence not visible in Fig. 1a. If needed, a further thermal oxidation step can also be performed to grow a 100-nm-thick conformal silicon dioxide layer, to be used as an insulation layer, on which a metal contact for actuation of the microgripper (or, in general, of the fabricated microsystem) can be deposited by quasi-conformal metal sputtering.

Sub-micrometer control of the silicon dissolution at the seed sites, in the *X*-*Y* plane and along the *Z*-direction, is obtained by properly modulating both the etching current density, J_{etch}, and the etching voltage, V_{etch}, as the etch progresses. The J_{etch} and V_{etch} values are kept within the working region: $J_{etch} < J_{peak}$ and $V_{etch} > V_{peak}$, where J_{peak} and V_{peak} represent the values of the current density and voltage of the electropolishing peak of the electrochemical system under investigation. In the working region, the silicon mass dissolved per unit time around a given *X*-*Y* position is proportional to the ratio J_{etch}/J_{peak} (also known as the porosity *P*), for any etching depth; the J_{peak} value also determines the etching rate in the *Z*-direction, which is, indeed, proportional to J_{peak}. The silicon dissolution (in terms of both volume and isotropy versus time) is finely tuned as the etching progresses by properly controlling the J_{etch} value over time. On the one hand, if the J_{etch} value is slowly reduced over time according to HF-diffusion kinetics, it is possible to compensate for the slight reduction of the J_{peak} value with etching depth, so that by maintaining the J_{etch}/J_{peak} ratio constant over time, the etching results to be perfectly anisotropic and, in turn, micromachined structures with excellent straight walls are achieved. The reduction of J_{peak} with etching depth is caused by a reduction in C_{HF} inside the etched trenches, due to stationary diffusion of HF molecules from the top to the bottom of the etched structures (Barillaro and Pieri 2005). On the other hand, if the J_{etch} value is suddenly increased over time with respect to the HF-diffusion kinetics, a dramatic decrease of the J_{peak} value occurs, which dynamically increases the J_{etch}/J_{peak} ratio, and, in turn, the silicon mass dissolved per unit time. A higher number of HF molecules per unit time, with respect to that supplied by stationary diffusion, is consumed at the bottom of the etched trenches as a consequence of the sudden increase of the J_{etch} value. The excess of HF molecule consumption leads to a dynamic reduction of the C_{HF} value and, in turn, of the J_{peak} value at the bottom of the etched trenches. The etching rate in the *Z*-direction, being proportional to J_{peak}, is therefore reduced, and the increased mass of silicon removed per unit time, J_{etch}/J_{peak}, mainly occurs in the *X* and *Y* directions, thus switching the etching from anisotropic to isotropic.

So far, ECM technology has been successfully applied to the fabrication of high-aspect-ratio microstructures and microsystems with application in different fields, from optofluidics (Barillaro et al. 2009b, 2011; Surdo et al. 2012) to biosensing (Merlo et al. 2012b, 2013; Surdo et al. 2012) and from photonics (Barillaro et al. 2007b, 2008, 2009a; Astrova et al. 2010; Polito et al. 2013; Surdo et al. 2013) to medicine (Merlo et al. 2012a, b; Strambini et al. 2012; Carpignano et al. 2012; Merlo et al. 2013). Figure 2 shows two examples of high-complexity microsystems fabricated by ECM technology. Figure 2a, b shows SEM images of MEMS structures consisting of freestanding inertial masses equipped with high-aspect-ratio comb fingers and suspended by high-aspect-ratio folded springs (AR about 100 for both fingers and springs) that are fixed to an anchor structure composed of a two-dimensional array of square holes (Bassu et al. 2012). In Fig. 2c, d, SEM images of an optofluidic platform consisting of two large reservoirs in

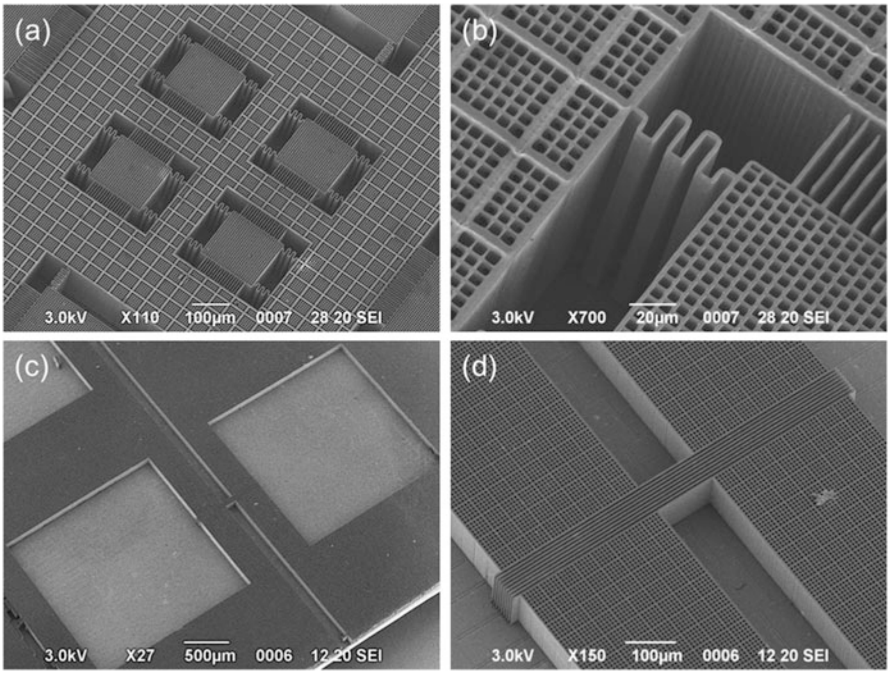

Fig. 2 Examples (SEM images) of two microsystems fabricated by ECM technology: (**a**) MEMS structures consisting of freestanding inertial masses suspended from the substrate by folded springs and featuring comb fingers for actuation; (**b**) magnification of a folded spring of the MEMS structures in (**a**); (**c**) optofluidic platform featuring a one-dimensional photonic crystal as sensing transducer; (**d**) magnification of the photonic crystal transducer of the platform in (**c**)

series to a high-aspect-ratio one-dimensional photonic crystal transducer for biosensing applications (detection of C-reactive protein (CRP) has been demonstrated) are shown (Surdo et al. 2012).

Summary

ECM technology enables the low-cost fabrication of high-complexity silicon microstructures and microsystems with sub-micrometer accuracy at aspect-ratio values (about 100) that are well beyond up-to-date, both wet and dry, micromachining technologies. Among ECM main features there are (i) fabrication of microstructure with very high aspect ratio, which can be three times higher than that of state-of-the-art deep etching techniques employed for microsystem fabrication; (ii) tunability of the etching anisotropy (from zero to one) in real-time as the etching progresses, which enables 3D freestanding microstructure fabrication by one-step etching; (iii) fine control of the etching features at the sub-micrometer scale, for both small (features down to 1 µm in size) and large (length over 1 mm) areas; and (iv) high quality of etched structures in terms of both verticality (percentage error over a depth of 100 μm of about 0.04 %) and surface roughness (about 20 nm). In the near future, ECM technology is expected to be greatly exploited at the lab scale, although not limited to, for silicon microstructuring, with potential impact on both microdevices and applications in different research fields.

References

Astrova EV, Nechitaĭlov AA (2008) Electrochemical etching of macropores in silicon with grooved etch seeds. Semiconductor 42:746–751

Astrova EV, Nechitailov AA, Tolmachev VA, Melnikov VA, Perova TS (2009) Photo-electrochemical etching of macro-pores in silicon with grooves as etch seeds. Phys Stat Solid A 206(6):1235–1239

Astrova EV, Tolmachev VA, Fedulova GV, Melnikov VA, Ankudinov AV, Perova TS (2010) Optical properties of one-dimensional photonic crystals fabricated by photo-electrochemical etching of silicon. Appl Phys A 98:571–581

Barillaro G, Pieri F (2005) A self-consistent theoretical model for macropore growth in n-type silicon. J Appl Phys 97:116105

Barillaro G, Strambini LM (2010) Controlling macropore formation in patterned n-type silicon: existence of a pitch-dependent etching current density lower bound. Electrochem Commun 12:1314–1317

Barillaro G, Nannini A, Pieri F (2002a) Dimensional constraints on high aspect ratio silicon microstructures fabricated by HF photoelectrochemical etching. J Electrochem Soc 149: C180–C185

Barillaro G, Nannini A, Piotto M (2002b) Electrochemical etching in HF solution for silicon micromachining. Sens Actuator A 102:195–201

Barillaro G, Diligenti A, Nannini A, Pennelli G (2003) A thick silicon dioxide fabrication process based on electrochemical trenching of silicon. Sens Actuator A 107:279–284

Barillaro G, Bruschi P, Diligenti A, Nannini A (2005a) Fabrication of regular silicon microstructures by photo-electrochemical etching of silicon. Phys Stat Solid (c) 2(9):3198–3202

Barillaro G, D'Angelo F, Pennelli G, Pieri F (2005b) Fabrication of self-aligned gated silicon microtip array using electrochemical silicon etching. Phys Stat Solid (a) 202(8):1427–1431

Barillaro G, Diligenti A, Benedetti M, Merlo S (2006) Silicon micromachined periodic structures for optical applications at $\lambda = 1.55$ μm. Appl Phys Lett 89(15):151110/1-3

Barillaro G, Nannini A, Piotto M (2007a) Electrochemical fabrication of buried folded microchannels into silicon substrates. Phys Stat Solid (a) 204(5):1464–1468

Barillaro G, Annovazzi-Lodi V, Benedetti M, Merlo S (2007b) Reflection properties of hybrid quarter-wavelength silicon microstructures. Appl Phys Lett 90(12):121110/1–121110/3

Barillaro G, Merlo S, Strambini L (2008) Band gap tuning of silicon micromachined 1D photonic crystals by thermal oxidation. IEEE J Sel Topic Quantum Electron 14(4):1074–1081

Barillaro G, Strambini LM, Annovazzi-lodi V, Merlo S (2009a) Optical characterization of high-order 1-D silicon photonic crystals. IEEE J Sel Topic Quantum Electron 15(5):1359–1367

Barillaro G, Merlo S, Strambini LM (2009b) Optical characterization of alcohol-infiltrated one-dimensional silicon photonic crystals. Opt Lett 34(12):1912–1914

Barillaro G, Merlo S, Surdo S, Strambini LM, Carpignano F (2011) Integrated optofluidic microsystem based on vertical high-order one-dimensional silicon photonic crystals. Microfluid Nanofluid 12:545–552

Bassu M, Surdo S, Strambini LM, Barillaro G (2012) Electrochemical micromachining as an enabling technology for advanced silicon microstructuring. Adv Funct Mater 22(6):1222–1228

Carpignano G, Silva S, Surdo V, Leva A, Montecucco F, Aredia AI, Scovassi S, Merlo G, Barillaro G, Mazzini G (2012) A new cell-selective three-dimensional microincubator based on silicon photonic crystals. PLoS One 7(11):e48556

Foll H, Carstensen J, Christophersen M, Hasse G (2000) Parameter dependence of pore formation in silicon within a model of local current bursts. Phys Stat Solid A 182:63–69

Kleimann P, Linnros J, Juhasz R (2001) Formation of three-dimensional microstructures by electrochemical etching of silicon. Appl Phys Lett 79:1727–1729

Köhler M (1999) Etching in microsystem technology. Wiley, Weinheim

Lehmann V (1993) The physics of macropore formation in low doped n-type silicon. J Electrochem Soc 140:2836–2843

Lehmann V (2002) Electrochemistry of silicon. Wiley, Weinheim

Lehmann V, Föll H (1990) Formation mechanism and properties of electrochemically etched trenches in n-type silicon. J Electrochem Soc 137:653–659

Matthias S, Müller F, Jamois C, Wehrspohn RB, Gösele U (2004) Large-area three-dimensional structuring by electrochemical etching and lithography. Adv Mater 16(23–24):2166–2170

Matthias S, Müller F, Schilling J, Gösele U (2005) Pushing the limits of macroporous silicon etching. Appl Phys A Mater Sci Process 80(7):1391–1396

Merlo S, Barillaro G, Carpignano F, Montecucco A, Leva V, Strambini LM, Surdo S, Mazzini G (2012a) Investigation of cell culturing on high aspect-ratio, three-dimensional silicon microstructures. IEEE J Sel Topic Quantum Electron 18(3):1215–1222

Merlo S, Barillaro G, Carpignano F, Silva G, Surdo S, Strambini LM, Giorgetti S, Nichino D, Relini A, Mazzini G, Stoppini M, Bellotti V (2012b) Fibrillogenesis of human β-microglobulin in three-dimensional silicon microstructures. J Biophotonics 5(10):785–792

Merlo S, Carpignano F, Silva G, Aredia F, Scovassi AI, Mazzini G, Surdo S, Barillaro G (2013) A new cell-selective three-dimensional microincubator based on silicon photonic crystals. Label-free optical detection of cells grown in 3D silicon microstructures. Lab Chip 13:3284

Ohji H, Trimp PJ, French PJ (1999) Fabrication of free standing structure using single step electrochemical etching in hydrofluoric acid. Sens Actuator A 73:95–100

Ottow S, Lehmann V, Föll H (1996) Processing of three-dimensional microstructures using macroporous n-type silicon. J Electrochem Soc 143:385–390

Polito G, Surdo S, Robbiano V, Tregnago G, Cacialli F, Barillaro G (2013) Two-dimensional array of photoluminescent light-sources by selective integration of conjugated luminescent polymers into three-dimensional silicon microstructures. Adv Opt Mater 1(12):894–898

Schilling J, Müller F, Matthias S, Wehrspohn RB, Gösele U, Busch K (2001) Three-dimensional photonic crystals based on macroporous silicon with modulated pore diameter. Appl Phys Lett 78(9):1180–1182

Strambini LM, Longo A, Diligenti A, Barillaro G (2012) A minimally invasive microchip for transdermal injection/sampling applications. Lab Chip 12:3370–3379

Surdo S, Merlo S, Carpignano F, Strambini LM, Trono C, Giannetti A, Baldini F, Barillaro G (2012) Optofluidic microsystems with integrated vertical one-dimensional photonic crystals for chemical analysis. Lab Chip 12(21):4403–4415

Surdo S, Carpignano F, Silva G, Merlo S, Barillaro G (2013) An all-silicon optical platform based on linear array of vertical high-aspect-ratio silicon/air photonic crystals. Appl Phys Lett 103 (17):171103